RSC Advances

ROYAL SOCIETY OF CHEMISTRY

www.rsc.org/advances

Fabrication and Gas sensitivity in heterostructures of Ortho – chloropolyaniline / ZnO nanocomposites

Syed Khasim[1, 2]* and Omar A Al-Hartomy[3]

[1]Department of Physics, Faculty of Science, University of Tabuk -71491, Saudi Arabia
[2]Department of Physics, PESIT-Bangalore South Campus, Bangalore-560100, India
[3]Department of Physics, Faculty of Science, King Abdul Aziz University – 21589, Jeddah, Saudi Arabia

Abstract: Recently the gas sensing properties of conducting polymer nano composites have been widely investigated. In this paper we report the fabrication of hetero junctions based on conducting ortho- chloropolyaniline/ Zinc oxide nanocomposites by in situ polymerization using sodium dodecylebenzene sulphonic acid and their potential towards gas sensing applications. The prominent peaks in FTIR spectra confirm the formation of nano composites. One dimensional growth of polymer fiber is observed through SEM and TEM with ZnO nanoparticles homogeneously distributed in the fiber matrix. The temperature dependent conductivity of the nano composites increases with increase in temperature as well as with the concentration of ZnO nanoparticles in the polymer matrix. This increase in conductivity is due to the hopping of charge carriers between the favorable sites. The synthesized nanocomposites were used to fabricate the sensor device on glass substrate with aluminum top electrodes. Gas sensing studies were carried out using two probe method in laboratory made sensor set up, it is observed that the 50 wt % of nanocomposites shows high sensitivity of 93 % at 400 ppm with fast response and small recovery time of 56.76 and 37.59 sec respectively. Reproducibility and stability study shows that these nano composites are highly stable. Selectivity study was carried out by passing different test gases and found that these composites show high sensitivity towards LPG.

Key words: Nanocomposites, Sensor device, Conducting polymer sensors, Gas sensors

Author of correspondence: syed.pes@gmail.com

1. Introduction

In recent years many sensors have been developed based on ceramic composites which operate at higher temperatures, this is a major problem for sensing the flammable gases. Over the last few years, there is a growing demand to fabricate the flammable gas sensors which works at room temperature, cost effective and easy to fabricate with high precession and reproducibility [1 – 3]. Many researchers are attracted towards fabrication of sensors using conducting polymer nanocomposites due to their tunable electrical properties by adding small amount of inorganic or organic fillers [4]. Many reports are available on polyaniline (PANI) metal oxide nano composites for liquid petroleum gas (LPG) sensors but it is observed that the hollow nanostructured polymer fibers shows higher sensitivity with fast recovery time due to high aspect ratio [5, 6]. A.S.Roy et al [7] reported that the sensitivity of substituted polyaniline is higher than pristine polyaniline and hollow fiber like geometry of the polymer is an added advantage for sensing of LPG.

Organic–inorganic-metal oxide/conducting polymer hybrid materials are currently of great interest for exploring enhanced sensor characteristics, due to their synergetic or complementary behaviors that is not available from their single counterparts [8 –10]. Much attention has been paid to investigate these kinds of hybrids for gas sensor applications. Lokhande et al. [11] have synthesized the polyaniline / CdS heterostructure, which has better sensitivity than the pristine CdS and polyaniline for LPG gas exposure. In this paper, we have made an attempt to prepare the Ortho-chloropolyaniline (OPANI) – Zinc Oxide (ZnO) nano composite fibers in different weight percentages and later characterized by XRD, FTIR, SEM and TEM. The dc conductivity studies were carried out using two probe method and the sensor device was fabricated on glass substrate to study the response of nanocomposites to LPG and

other test gases.

2. Experimental

2.1 Preparation of zinc oxide nanoparticles

The precursor zinc oxalate is prepared by mixing solution of 0.1M zinc chloride and oxalic acid (0.1M). The precipitate of zinc oxalate obtained is filtered and washed with distilled water and dried under vacuum. The dried precursor is grinded into a fine powder using agate motor and weighed. The known quantity of powder precursor is mixed with finely powdered polyethylene glycol (PEG) in the ratio of 1:5. The mixed precursor and PEG is placed in a china dish and heated in the presence of air. It is observed that the PEG first melts and forms froth and ignites to form nanosized ZnO. The nanosized zinc oxide is sonicated in acetone media for 20 min and then calcinated at 300 °C to remove the impurities. Finally, fine graded pure nanosized zinc oxide particles are formed [12, 13].

2.2 Synthesis of PANI using sodium dodecyl benzene sulphonic acid (SDBSA)

10 ml of monomer aniline is dissolved in equimolar amount of concentrated hydrochloric acid and is cooled to – 3 °C for 30 min. Ammonium peroxydisulphate (APS) and sodium dodecylebenzene sulphonic acid (SDBSA) are also taken in equimolar ratio with respect to aniline hydrochloride. First, sodium dodecylebenzene sulphonic acid is added to ortho chloroaniline - hydrochloride drop wise followed by drop wise addition of APS to form ortho-chloro polyaniline. The reaction mixture was kept under ice medium at -5 °C for 48 hours [14]. A smooth jelly like reaction mixture was vacuum filtered under high pressure, the precipitate was washed first with acetone and then sonicated for 20 minute to remove oligomers and then

the precipitate was vacuum filtered and washed with deionised water. Finally, the resultant precipitate was dried for 24 h to achieve a constant weight [15, 16].

2.3 Substituted Ortho-chloropolyaniline / ZnO nanocomposites

Syntheses of OPANI / ZnO nanocomposites have been carried out by in situ polymerization technique. 0.1 mol of *O*-chloroaniline was dissolved in 1 M HCl to form *O*-chloroaniline hydrochloride. Zinc oxide prepared by above discussed method is added in different weight percent with vigorous stirring in order to keep the ZnO suspended in the solution. To this mixture, 0.1 M of ammonium persulphate [$(NH_4)_2S_2O_8$] which acts as oxidant and sodium dodecylebenzene sulphonic acid (SDBSA) was added drop wise slowly with continuous stirring for 4 hrs at 5 °C to polymerize ortho chloroaniline. The precipitate was filtered, washed with deionized water and finally dried in an oven for 24 hrs to achieve a constant weight. In this way, OPANI / ZnO nanocomposites of various weight percentages of ZnO (10, 20, 30, 40 and 50) in OPANI were synthesized [17].

The pellets of 10 mm diameter and 2 mm thickness are prepared by applying pressure of 10 Tons in a UTM – 40 (40 Ton Universal testing machine). For the study of temperature dependent conductivity, the pellets are coated with silver paste on either side of the surface to obtain better contacts [18].

2.4 Design of Gas Sensor set up

The sensors set up consist of rectangular glass box of dimension of 6 x 8 x 18 inches with a total volume of 14,158 cm^3 as shown in figure 1. F1, F2, F3 and F4 refer to flow meters used to introduce different test gases in to the chamber through the gas balloon, where the test gases mix with each other [19]. The chamber is provided with a heating element to increase the temperature

of the sample, in the present study only room temperature measurement has been carried out. The change in electrical resistance was recorded by two probe method using Keithley – 2000 digital multimeter as shown in figure 1. The degasification (evacuation of gases) was done by connecting vacuum pump to the out let.

2.5 Fabrication of sensor device

The gas sensor device used in the present study was designed and fabricated to operate as a conductometric gas sensor. The device has two important physical components: sensitive layer which interacts with the analite and transducer which converts the chemical sensor to an electrical sensor [20]. The active layers of sensor were composite of ZnO nanoparticles and Ortho-chloropolyaniline.

To form the heterojunctions, OPANI – ZnO nanocomposites were prepared by in situ polymerization method [21] and the powders were directly added into DMPU and stirred for 2 hours to form homogeneous solution which is used to prepare thin films on a glass substrate. Five different composite thin films were prepared through spin coating technique on 25 mm × 25 mm glass substrate. Pristine Ortho-chloropolyaniline films were also prepared as reference samples to compare the results. The aluminum electrodes were deposited on the film surface to form a transducer at room temperature by thermal vacuum deposition technique. The working pressure of vacuum chamber was maintained at 10^{-6} mbar. Tungsten (W) coil was used for evaporating the source material, the substrates were cleaned by acetone, isopropanol and distilled water respectively and dried with ultra pure argon gas (Ar). The source-substrate distance of 12cm was maintained for all samples [22 – 23]. The thickness and evaporation rate were monitored by quartz crystal monitor. The gas sensing device prepared using OPANI-ZnO nano composite hetero structure is shown in figure 2.

3. Results and discussion

3.1 X – rays diffraction (XRD) :

Figure 3 (a – c) shows the X-ray diffraction (XRD) patterns of OPANI (Fig 3a), ZnO (Fig 3b) and OPANI / ZnO nano composites with 50 wt % of ZnO in ortho chloropolyaniline (Fig3c). By comparing the XRD pattern of composite (Fig 3c) with that of ortho chloropolyaniline (Fig 3a), the prominent peaks corresponding to 2θ = 28. 3°, 30.6°, 33.1°, 44.5°, 53.1°, 59.6°, 65.3° and 74.5° are due to (1 0 0). (0 0 2), (1 0 1), (1 0 2), (1 1 0), (1 0 3), (1 1 2) and (2 0 2) planes of ZnO (JCPDS No: 36-1451). By comparing the XRD patterns of the composite (Fig 3c) with pure ZnO (Fig 3b), it is confirmed that ZnO nano particles have retained their structure even though it is dispersed in ortho chloropolyaniline during polymerization reaction. It is interesting to note that when the XRD pattern of composite is compared with ZnO diffraction pattern, the broad peaks shifted to lower side due to the vanderwaal's interaction between OPANI and ZnO.

3.2 Fourier transform infrared spectroscopy (FTIR):

Figure 4 (a) shows the FTIR spectra of pure ortho chloropolyaniline. The important peaks observed at 601 cm^{-1} corresponds to C-H out of plane bending vibration, 756 cm^{-1} is due to the chloro group attached to the phenyl ring, 1058 cm^{-1} is assigned to C- O-C stretching, 1211 cm^{-1} is due to C-H in plane bending, 1444 cm^{-1} for C-N stretching of benzenoid rings, 1578 cm^{-1} for C-N stretching of quinoid rings and 3194 cm^{-1} for N-H stretching vibration. These observed peaks confirm the formation of ortho choloropolyaniline [24, 25].

The FTIR spectra of ortho OPANI /ZnO nanocomposites of various weight percentages (10, 20, 30, 40 and 50 wt %) are shown in figure 4 (b-f). The prominent peaks that are observed in OPANI / ZnO nanocomposites are 594 - 599 cm^{-1} which corresponding to C-H out of plane bending vibration, 750 – 754 cm^{-1} is due to the chloro group attached to the phenyl ring, 833 – 889 cm^{-1} is due to ortho disubstituted aromatic rings indicating polymerization, 1055cm^{-1} is assigned to C- O-C stretching, 1086 – 1089 cm^{-1} corresponds to C-H in plane bending, 1294 cm^{-1} - 1297 cm^{-1} for aromatic C-N stretching indicating secondary aromatic amine group, 1440 -1444 cm^{-1} for C-N stretching of benzenoid rings and 1571 – 1578 cm^{-1} corresponds to C-N stretching of quinoid rings [26]. The careful observation of FTIR reveals that the characteristic stretching frequencies are considerably shifted towards lower frequency side as in case of OPANI/ ZnO nanocomposites, which suggest a Vanderwaal's kind of interaction between the polymeric chain and ZnO nano particles.

3.3 Scanning electron microscopy (SEM)

Figure 5 (a-f) shows the SEM images of OPANI-ZnO Nano composites, *O*-chloropolyaniline prepared by using *Ortho*-phosphoric acid shows that the grains are agglomerated and spherical in shape as shown in figure 5 (a). The average grain size is found to be about 0.5μm. Since HCl is used as protonic acid in the preparation of ortho chloropolyaniline, the presence of microcrystalline structure can be seen. The presence of microcrystalline structures in ortho chloropolyaniline in these particular samples can be confirmed from the XRD studies.

Figure 5 (b) shows the SEM image of 10 wt % of OPANI / ZnO nano composite. It is found that the fiber like structures begin to form in OPANI / ZnO nano composite. These fibers

are horizontally interconnected with each other forming the bundle like structure. The average length of fiber is found to be 1 to 2.3 μm. Figure 5 (c) shows the SEM image of 20 wt % of OPANI / ZnO nanocomposites. It is found that the fibers are more agglomerated compared to 10 wt% composite. Figure 5 (d) shows the SEM image of 30 wt % of OPANI / ZnO nanocomposites. It is observed that the fibers are highly clustered, irregular in shape and exhibit branched like structure. The average length of the fibers is found to be 1.7μm. Figure 5 (e) shows the SEM image for 40 wt % of OPANI / ZnO nanocomposites. The fibers are highly clustered, irregular in shape and exhibit branch like morphology and are well interconnected with each other. It is observed that the fibers are attached parallel to each other and the average length of the fiber is found to be 1.9 μm. Figure 5 (f) shows the SEM image of 50 wt % of OPANI / ZnO nanocomposites. It is found that the composites are formed with a spike like structures, regular in length and interconnected with each other. These spikes are hollow cylindrical in nature where in nanosized zinc oxide are embedded in polymer matrix. Some of the agglomerated oxide particles are found attached along with the composites fibers. The average length of the fibers is found to be 1.3μm.

3.4 Transmission electron microscopy (TEM)

The TEM image of pure ZnO (Fig 6a) shows the presence of spherical shaped nanoparticles. The surface to volume ratio of ZnO nanoparticles decreases the size of ZnO from bulk to nano. The size of ZnO nanoparticles was found to be 13 nm. The spherical morphology of ZnO nanoparticles with high aspect ratio helps in sensing mechanism. The TEM image of OPANI / ZnO nanocomposite is as shown figure 6 (b) indicates a tubular structure with ZnO nano particles embedded in polymer matrix. The hallow tubular structure is formed due to the high aspect ratio of ZnO nanoparticles which initiates the nucleation in two dimensions. The

length of the tubular structure is found to be 250 nm and diameter is about 73 nm where in ZnO nanoparticles of 13 nm are found embedded. The tubular morphology with embedded ZnO nano particles helps the gas under test to penetrate through porous region of tubular structure, leading to higher sensitivities due to curling and uncurling of polymer chains.

4. DC Conductivity

Figure 7 shows the variation of dc conductivity as a function of temperature for different wt% of ZnO nanoparticles in Ortho-chloropolyaniline. It is observed that, conductivity of these composites increases exponentially with temperature as well as with weight percentages of ZnO. The conductivity was measured in the temperature range from 30 °C to 220 °C, the observed response shows a three step conductivity due to one dimensional variable hopping of charge carriers as per Mott theory. It is found that, the conductivity remains constant up to 80 °C for OPANI and other nanocomposites, after 80 °C it increases exponentially till 170 °C later it shows sudden increases up to 220 °C [27, 28]. The increase in the conductivity at higher temperature is due to extended chain length of ortho chloropolyaniline which facilitate the hopping of charge carriers when the content of ZnO nanoparticles is up to 50 wt %. Further the decrease in conductivity at lower temperature is observed which may be attributed to the non-uniform distribution of ZnO nanoparticles causing larger grain boundaries and resulting in partial blocking of the hopping of charge carriers [29]. From Fig.7 it is also observed that that the conductivity of 10wt% composite is less than the pure OPANI. This ambiguity is mainly due to thermal agitations (Grain boundary strains) and most common phenomena in organic/inorganic hybrid composites for the initial concentration of metal oxides dispersed in polymer matrix. Similar results have been observed in many organic/inorganic composite systems (disordered systems), where this ambiguity is observed for initial content of metal oxide in polymer matrix

[30-35]. The conductivity increases further for higher concentration (20 wt% and above) of metal oxide in OPANI due to the formation of favorable conduction path that facilitates the hopping of charge carriers.

5. Sensor study

5.1 Gas sensing mechanism

The gas sensing mechanism in OPANI – ZnO nanocomposites is expected mainly because of two reasons. First the trapping of gas molecules in between the OPANI – ZnO nano composite islands by electrostatic forces and second is a surface controlled phenomenon i.e., it is based on the change in surface resistance of the nanocomposites at which the gas adsorb and reacts with pre-adsorbed oxygen molecules [36]. The OPANI – ZnO nanocomposites film is more porous due to the distribution ZnO nanoparticles in the tubular structure (as observed from TEM). Therefore, the oxygen chemisorptions centers viz., oxygen vacancies, localized donor and acceptor states and other defects are formed on the surface during synthesis. These centers are filled by adsorbing oxygen from atmospheric air. When the composites film is placed inside the gas sensing setup, after some time equilibrium is established between oxygen adsorbed at the surface of sensing element and atmospheric oxygen through the chemisorptions at room temperature. The stabilized resistance at this state is known as resistance in the presence of air (Ra). The electron transfer from the conduction band to the chemisorbed oxygen results in the decrease of electron concentration at the film surface [37, 38]. As a consequence, a decrease in the resistance of the film is observed. In LPG, the reducing hydrogen species are bound to carbon, therefore, LPG dissociates less easily into the reactive reducing components on the film surface. When the film is exposed to reducing gas like LPG, it reacts with the chemisorbed oxygen and is adsorbed on the surface of the film then the exchange of electrons take place

between the LPG and oxide surface upon adsorption i.e., a surface charge layer will be formed. When the LPG reacts with the surface oxygen ions of the nanocomposites, a potential barrier would be developed i.e., this mechanism involves the displacement of adsorbed oxygen species by formation of water [39]. The overall reaction of LPG with the chemisorbed oxygen may take place as shown in figure 8.

In figure 8, the C_nH_{2n+2} represent the various hydrocarbons. The free electrons released through reaction between the LPG molecules and the pre-adsorbed O^{2-} neutralize the holes, which are the majority carrier in n-type ZnO nanoparticles. This compensation results in decrease of hole carrier concentration in composites, and consequently, an increase in sensor resistance was observed. Here the oxygen molecules are continuously supplied from the dilution gas (dry air) and are adsorbed on the OPANI – ZnO nanocomposite surface. When the flow of LPG is stopped for recovery, the oxygen molecules present in air will adsorb on the surface of OPANI – ZnO nanocomposites and the capture of electrons through the processes indicated in equations (fig 8) will reduce the surface resistance of the sensor during initial stage. In the first cycle of exposure, LPG molecules interact with the pre-adsorbed oxygen on the surface of OPANI – ZnO nanocomposite and the sensor resistance increases. Since the sensing mechanism of this devices is based on the chemisorption reaction that take place at the surface of the polymer and metal oxide, increasing specific surface area of the sensitive materials leads to more sites for adsorption of surrounding gases.

Figure 9 shows the change in sensitivity with concentration of LPG in parts per million at constant volume (ppm_v) for pure ortho - chloropolyaniline at room temperature (25 °C). It is observed that, when the films were exposed to a gas, the polymer matrix swells. The increase in

volume causes a decrease in resistance due to disturbed conductive pathways through the material. When the gas is released, the polymer chains returns to their original size, restoring the conductive pathways. Thus the sensitivity increases with increase in the concentration of the gas. In contrary to DC conductivity studies, the sensitivity of 10 wt% composite increases in comparison to pure OPANI, which is mainly due to creation of more number porous sites by the addition of metal oxide that facilitate gas molecules to penetrate into polymer matrix and reaction mechanism shown in Fig 8 leads to enhancement of sensitivity. As the content of metal oxide in polymer matrix increases, it leads to formation of more porous sites and hence the observed sensitivity increases for all the composites. Among different OPANI / ZnO nanocomposites, 50 wt% composite shows maximum change in sensitivity when compared to pure OPANI, 40, 30, 20 & 10 wt % composites. The enhanced sensitivity for 50 wt% composite is expected due to the formation of conducting pathway which facilitates the hopping charge carriers more favorably.

Figure 10 shows the response and recovery curve as a function of time for OPANI and OPANI / ZnO nanocomposites respectively. It is observed that, the sensitivity lies between 10 to 95 % at 400 ppm for 50 wt % of OPANI / ZnO nanocomposites, where as for OCPANI and 40, 30, 20 and 10 wt % composites sensitivity lies between 23 and 58%. The response and recovery curves with time for the OPANI and OPANI/ZnO nanocomposites are shown in table 1. Among all nanocomposites, it is observed that 50 wt % composite shows fast response time and small recovery time of 56.76 and 37.59sec respectively which may be due to the nucleation of single folded sheet of polymer over the ZnO nanoparticles results into hollow fiber nanocomposites favorable for absorption of LPG. However, the reproducibility with high precession sensing response of these nanocomposites are the major issue, therefore we made an attempt to study the

sensitivity of the fabricated device by using 50 wt % of OPANI – ZnO nanocomposites. In different time of interval (30, 60 and 90 days) the device is exposed to the LPG for five cycles and its sensitivity was measured as shown in figure 11. It is observed that these nanocomposites are highly stable and produce similar sensitivity even after 90 days but the surface gets saturated after exposing the LPG for 80 seconds, hence these nanocomposites are highly potential for fabrication of flammable gas sensor for domestic uses as well as in industrial application.

Figure 12 shows the variation of selectivity of the OPANI/ZnO nanocomposites for various gases such as Benzene, trichloroethylene, Cyclohexane and LPG at 400 ppm. It is expected here that different gases would produce different resistance response that depends on catalytic activity of ZnO nanoparticles. This could be used as a means to selectively distinguish between different gases. It can be seen that the response for Benzene and trichloroethylene are negligibly small (≤ 20%) and for Cyclohexane, the sensing response is less than 30% for different wt % composites, where as for LPG the maximum sensing response is found to be 93 % for 50 wt % of OPANI – ZnO nanocomposites at 400 ppm. The increase in sensitivity and selectivity of OPANI / ZnO nanocomposites is due to hallow tubular nanostructure which is more sensitive and reactive in LPG environment.

6. Conclusion

Ortho- chloropolyaniline / ZnO nanocomposites have been prepared by in situ polymerization using sodium dodecylebenzene sulphonic acid. The prepared nanocomposites were characterized by XRD and FTIR for structural properties and SEM, TEM to study surface morphology. The formation of nanocomposites is confirmed by FTIR spectra where the

important peaks are observed like benzenoid, quinoid ring and metal oxide stretching. The ortho chloroaniline nucleation occurs in one dimension due to the surface tension created by sodium dodecylebenzene sulphonic acid surfactant and it is observed in SEM. It is also observed that the ZnO nanoparticles are homogeneously distributed in the fiber matrix. In TEM image it is found that the ZnO nanoparticle size is about 13 nm and it is embedded in the ortho chloropolyaniline matrix. DC conductivity shows the increase in conductivity with increase in temperature as well as content of ZnO nanoparticles in polymer matrix. Among all composites 50 wt % shows the highest conductivity of 0.004 S/cm and this increase in conductivity is due to the favorable hopping of charge carriers. Further the synthesized nanocomposites were used to fabricate the sensor device on glass substrate with the top electrodes prepared by Al powder using physical vapor deposition technique. The sensor study was carried by two probe sensor set up and it is observed that the 50 wt % of OPANI-ZnO nanocomposite shows high sensitivity of 93 % at 400 ppm with fast response and small recovery time of 56.76 and 37.59 respectively. Reproducibility and stability study shows that these nanocomposites are stable upto 60 days and can be used upto five cycles with high sensitivity. Selectivity study was carried out by passing test gas into the sensing chamber and found that among different test gases, LPG shows highest sensitivity. Therefore these nanocomposites have great applications in gas-sensor technology in particular for flammable gases.

References

[1] K. Arshak, I. Gaidan, Mater. Sci. Eng. B 118, 44 (2005).

[2] V.R. Shinde, T.P. Gujar, C.D. Lokhande, Sens. Actuators B 120, 551(2007).

[3] L.F. Nazar, Z. Zang, D. Zinkweg, J. Am. Chem. Soc. 114, (1992) 6239

[4] G. Cao, M.E. Garcia, M. Aleala, L.F. Burgess, T.E. Mallouk, J. Am. Chem. Soc. 114, (1992) 7572

[5] L.L. Beecreft, C.K. Ober, Chem. Mater. 9, (1999) 1302

[6] P.R. Somani, R. Marimuthu, U.P. Mulik, S.R. Sainkar, D.P. Amalnerkar, Synth. Met. 106, (1999) 45

[7] A. S. Roy, T Machappa, M.V.N Sasikala, M. V. N. Ambika Prasad, Sensor letter, 9, (2011) 1

[8] A. Khan, A. S Aldwayyan, M. Alhoshan, M. Alsalhi, Polym Int, 59 (2010)1690

[9] Z. Zhang, D. Pan, J. Feng, L. Guo, L. Peng, C. Xi, J. Li, Z. Li, M. Wu, Z. Ren, Materials letter, 66 (2012) 54

[10] S. Maeda, R. Corradi, S.P. Armes, Macromolecules, 28, (1995) 2905

[11] D.S. Dhawale, D.P. Dubal, V.S. Jamadade, R.R. Salunkhe, S.S. Joshi, C.D. Lokhande, Sensors and Actuators B 145 (2010) 205–210

[12] G.P. Mccarthy, S.P. Armes, S.J. Greaves, J.F. Watts, Langmuir; 13 (1997) 3686

[13] S.L. Patil, M.A. Chougule, S. Sen, V.B. Patil, Measurements 45 (2012) 243–249

[14] K. Ogura, N. Endo, S.J. Kuvabata, Electrochem. Soc. 145 (1998) 3801

[15] H.S. Xia, Q. Wang, Chem. Mater. 14, (2002) 2158

[16] L. Zhang and M. Wan, J. Phys. Chem. B, 107 (2003) 6748

[17] H.S. Xia, Q. Wang, J. Appl. Polym. Sci, 87 (2003) 1811

[18] G. Gustafsson, Y. Cao, G.M. Treacy, F. Klavetter, N. Colaneri, A.J. Heeger, Nature, 357, (1992) 477

[19] A. Parveen, A. R. Koppalkar, A. S. Roy, Sensor Letters, 11, (2013) 242

[20] N. T. Tung, T. V. Khai, H. Lee, D. Sohn, Synthetic Met, 161, (2011) 177

[21] W. Gopel, D. Schierbaum, Sens. Actuators B, 26, (1995) 1

[22] S Maeda, S. P. Armes, Chem. Mater. 7, (1995) 171

[23] S. Santucci, L. Lozzi, M. Passacantando, S. Di Nardo, A. R. Phani, C. Cantalini and M. Pelino. J. Vacuum Sci. Tech A, 17, (1999) 644

[24] C. Cantalini, W. Wlodarski, H.T. Sun, M.Z. Atashbar, M. Passacantando, A.R.Phani, S. Santucci, Thin Solid Films; 350, (1999) 276

[25] R. Liu, H. Qiu, H. Li, H. Zong, C. Fang, Synth Met, 160, (2010) 2404

[26] N. Gospodinova, L. Terlemezyan, Prog. Polym. Sci. 23, (1998) 1443

[27] Y. Li, J. Gong, G. He, Y. Deng, Synth Met, 161, (2011) 56

[28] Z. Wang, X. Hu, Electrochemica Acta; 46, (2001) 1951

[29] B. O'Regan, M. Gratzel, Nature; 353, (1991) 737

[30] Aashish S Roy, Ameena Parveen, M V N Ambika Prasad, Kopalkar R Anilkumar, Sensor Review; 32 (2013) 163-169

[31] Ameena Parveen, Anilkumar R Kopalkar, Aashish S Roy, IEEE Sensor Journal, 12 (2012) 2817-2823

[32] Aashish S Roy, Kopalkar R Anilkumar, M V N Ambika Prasad, J.Appl.Poly.Sci. 123 (2012), 1928-1934

[33] Ameena Parveen, Anilkumar R Kopalkar, Aashish S Roy, Sensor Letters, 9, (2011), 1342-1348

[34] Ramesh Patil, Aashish S Roy, Kopalkar R Anilkumar, J.Appl.Poly.Sci, 121, (2011), 262-266

[35] Muhammad Faisal, Syed Khasim, Bull. Korean Chem. Soc. 34, (2013), 99-106

[36] M. Machida, K. Norimoto, T. Watanabe, K. Hashimoto, A. Fujishima, J. Mater. Sci. 34, (1999) 2569

[37] H. Zhang, R. Zong, Y. Zhu, J. Phys. Chem. C, 113, (2009) 4605

[38] B.C. Yadav, R. Srivastava, A. Yadav and V. Srivastava, Sens. Letters 6, (2008) 714

[39] V.R. Shinde, T.P. Gujar, C.D. Lokhande, Sens. Actuators B; 120, (2007) 551

Figure captions:

1. Figure 1: The gas-sensor set up
2. Figure 2 Schematic Fabrication of sensor device on glass substrate
3. Figure 3 (a – c): XRD spectra of pure ortho chloropolyaniline (a), ZnO nanoparticles (b) and ortho chloropolyaniline – ZnO nanocomposites (c)
4. Figure 4 (a – f): FTIR spectra of pure ortho chloropolyaniline, ZnO nanoparticles and ortho chloropolyaniline – ZnO nanocomposites for various weight percentages
5. Figure 5 (a – f): SEM image of pure ortho chloropolyaniline, ZnO nanoparticles and ortho chloropolyaniline – ZnO nanocomposites for various weight percentages

6. Figure 6 (a, b): TEM image of ZnO nanoparticles and 50 wt % of ortho chloropolyaniline – ZnO nanocomposites
7. Figure 7 DC conductivity of ortho chloropolyaniline and ortho chloropolyaniline – ZnO nanocomposites for various weight percentages
8. Figure 8 Schematic representation of LPG gas sensing mechanism
9. Figure 9 Variation of sensitivity as a function of concentration of gas for nanocomposites
10. Figure 10 Response and recovery curve for nanocomposites
11. Figure 11 Reproducibility and stability of ortho chloropolyaniline and ortho chloropolyaniline – ZnO nanocomposites
12. Figure 12 Sensitivity of nanocomposites for various test gases

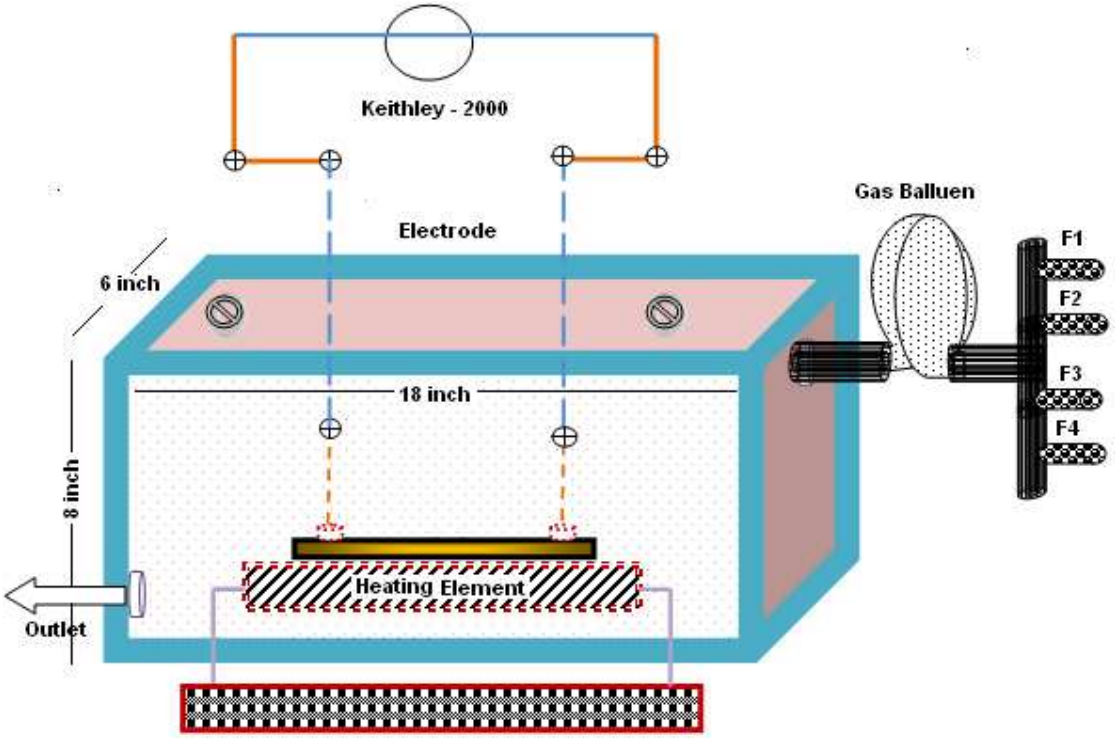

Figure 1

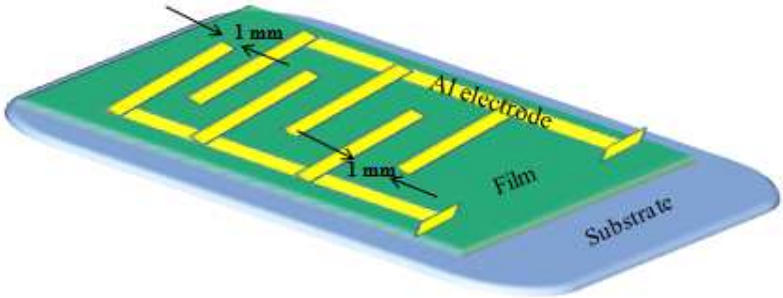

Figure 2

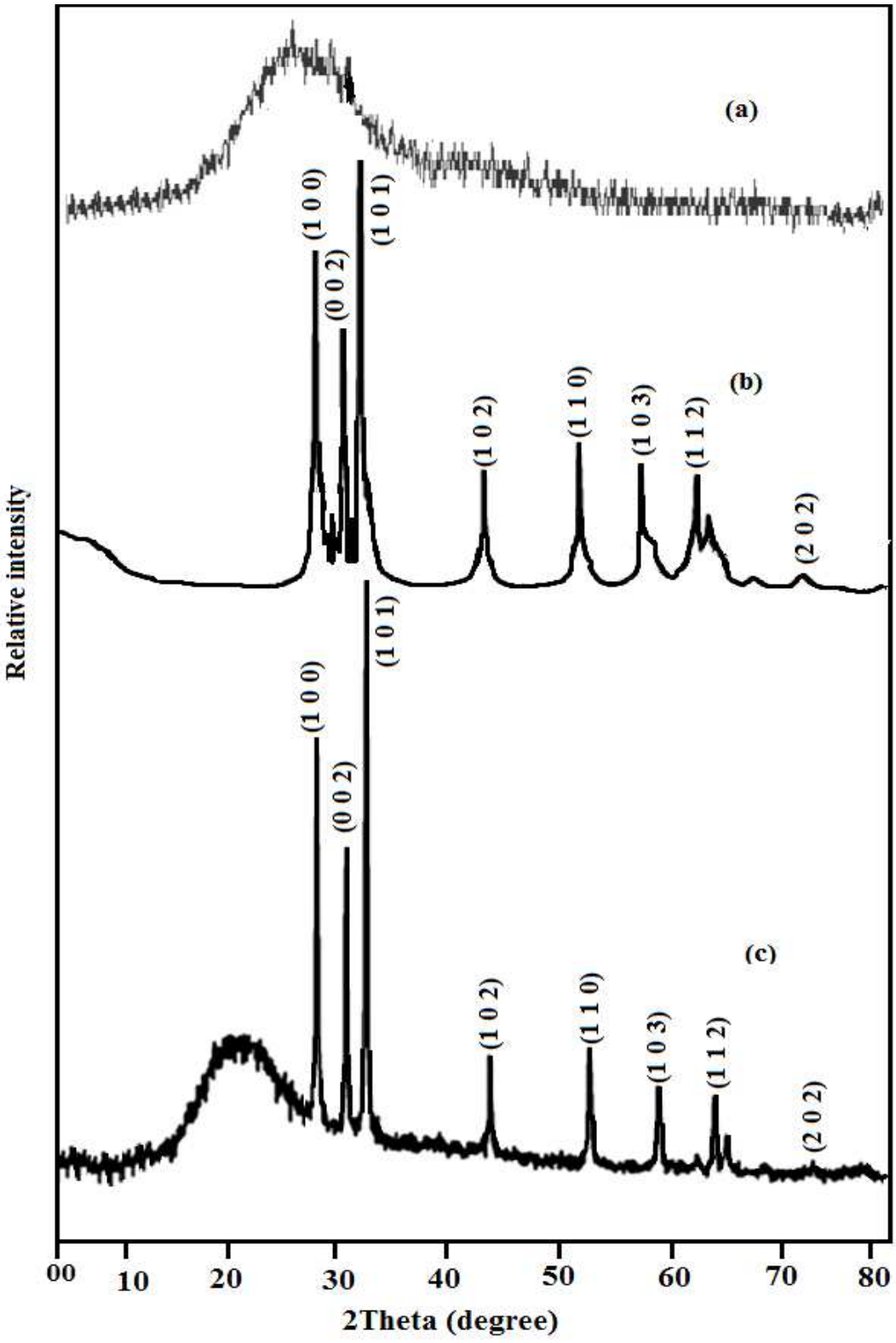

Figure 3 (a – c)

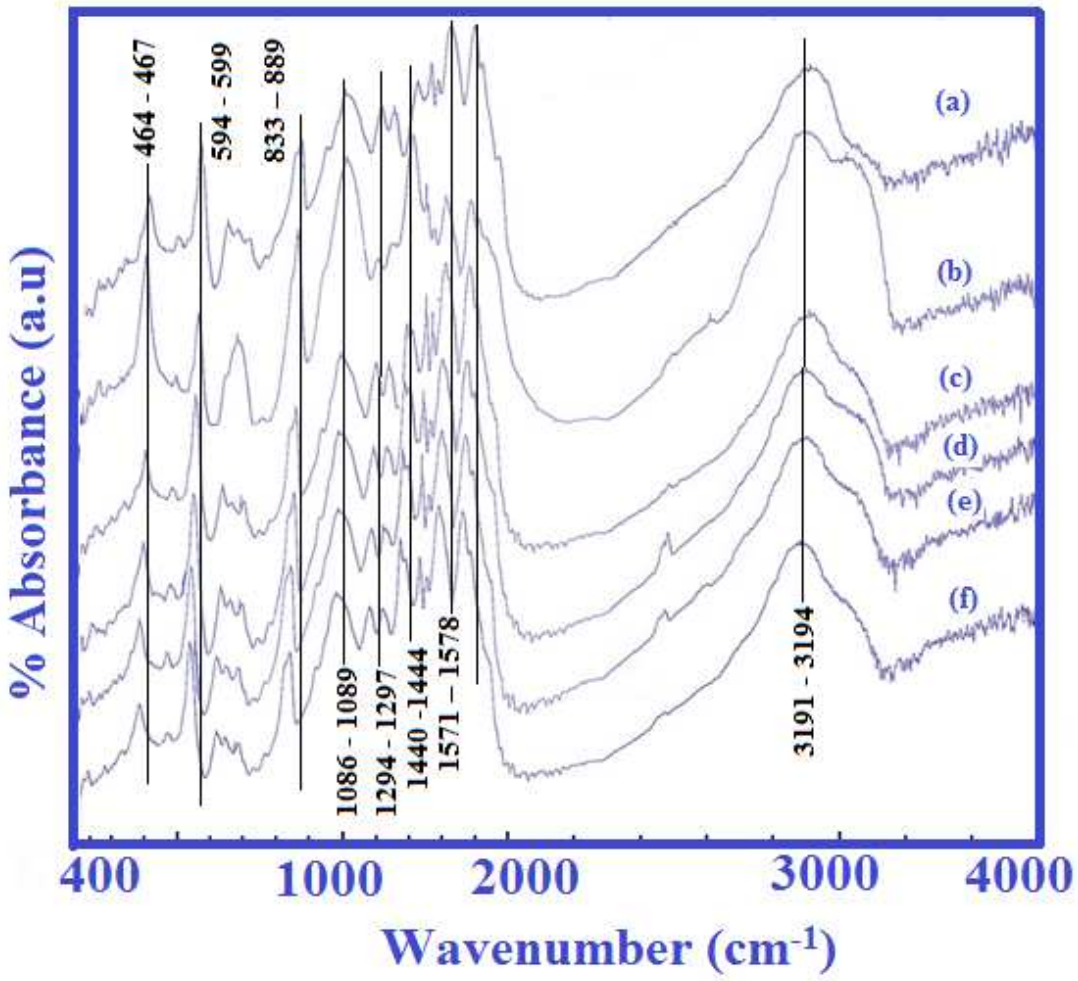

Figure 4 (a – f)

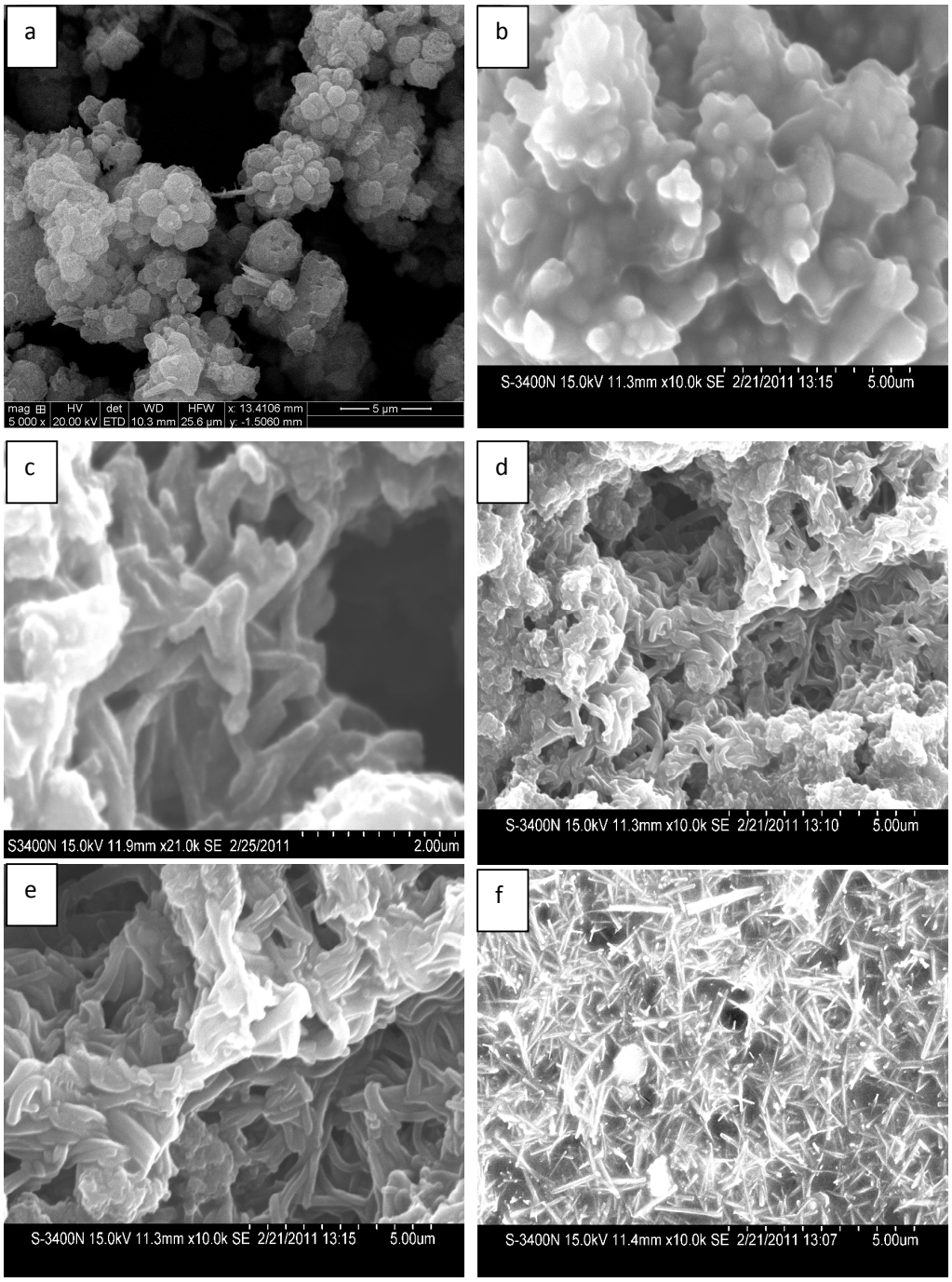

Figure 5 (a-f)

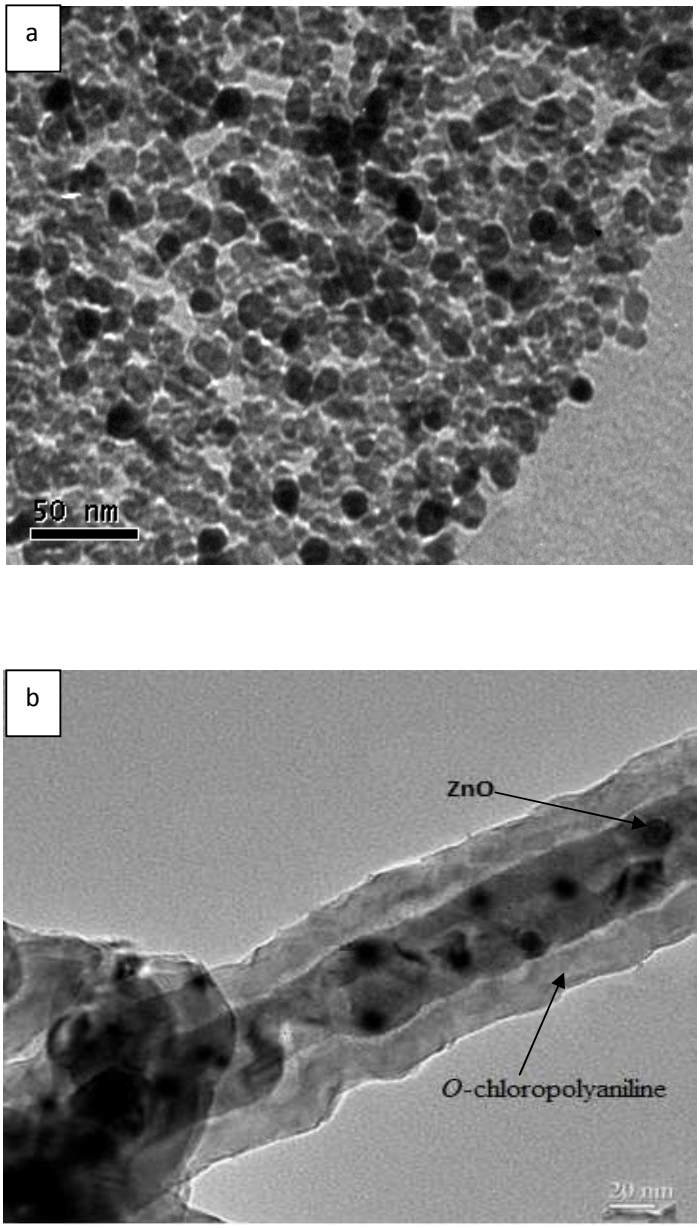

Figure 6 (a and b)

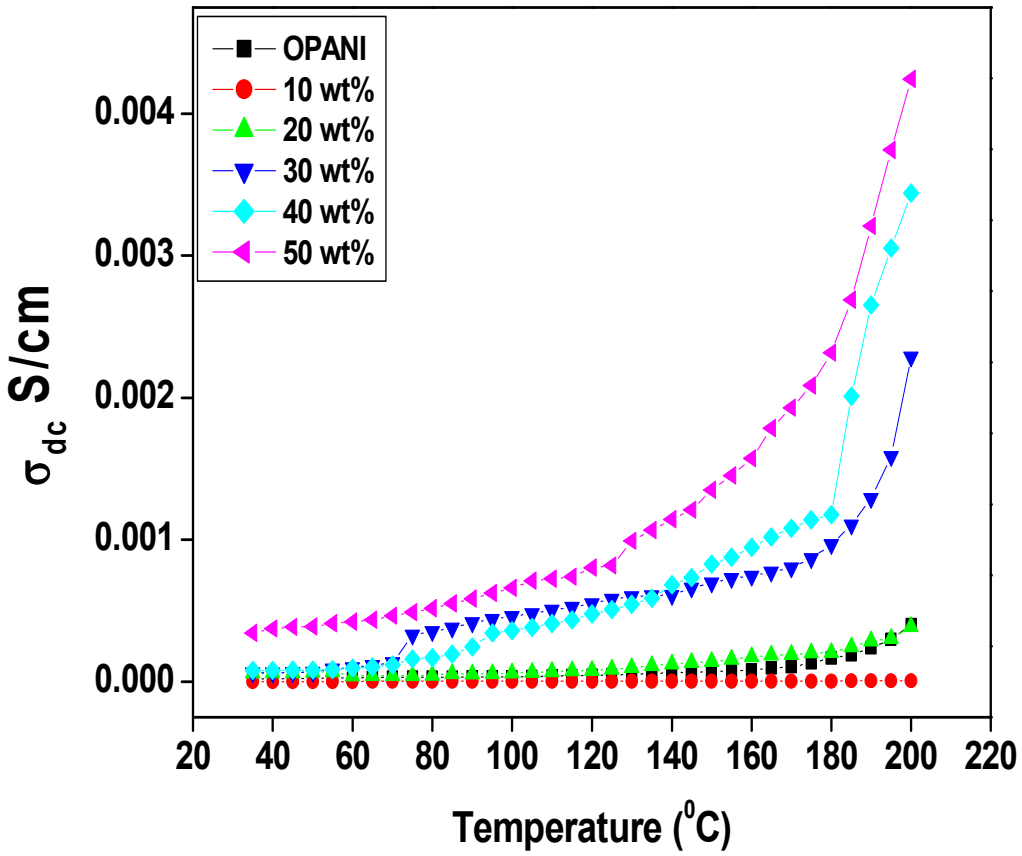

Figure 7

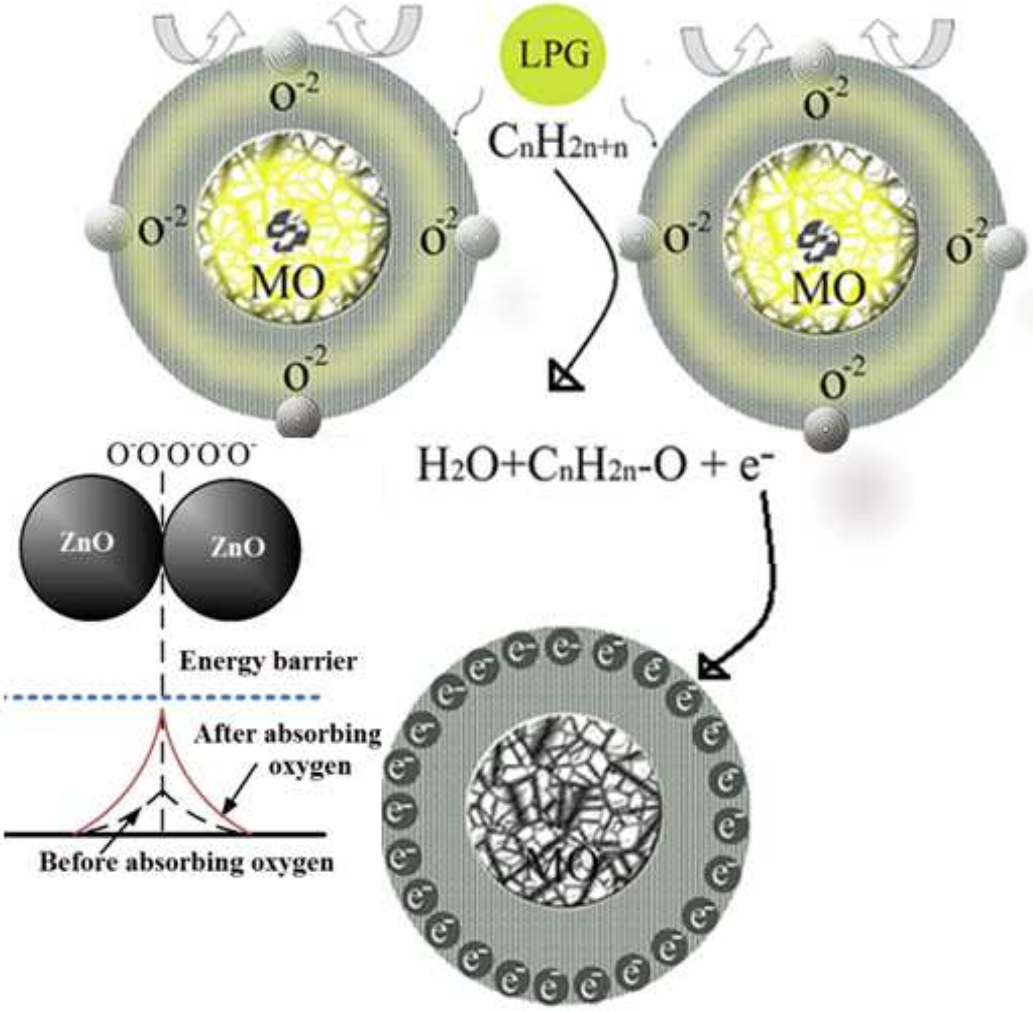

Figure 8

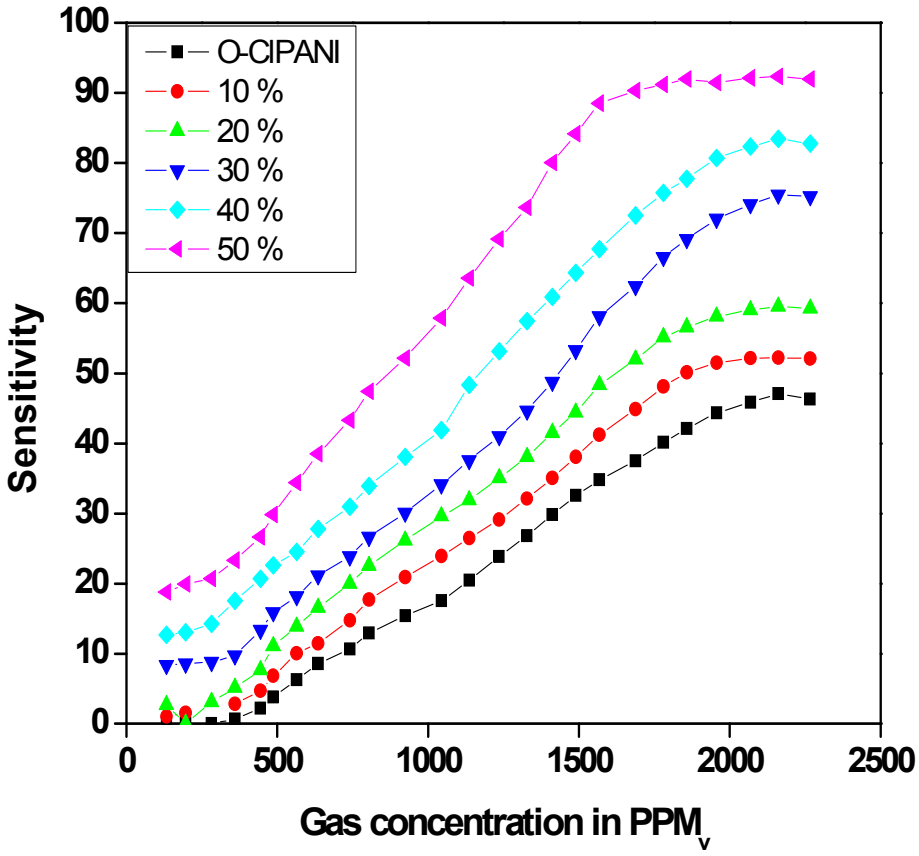

Figure 9

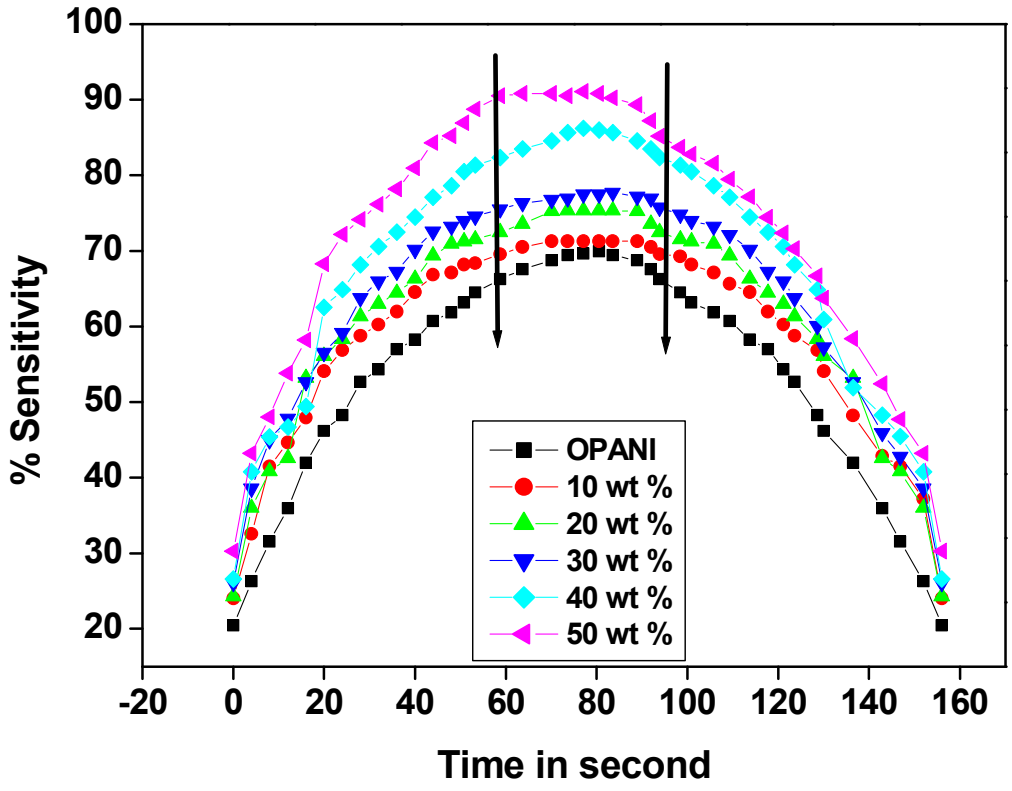

Figure 10

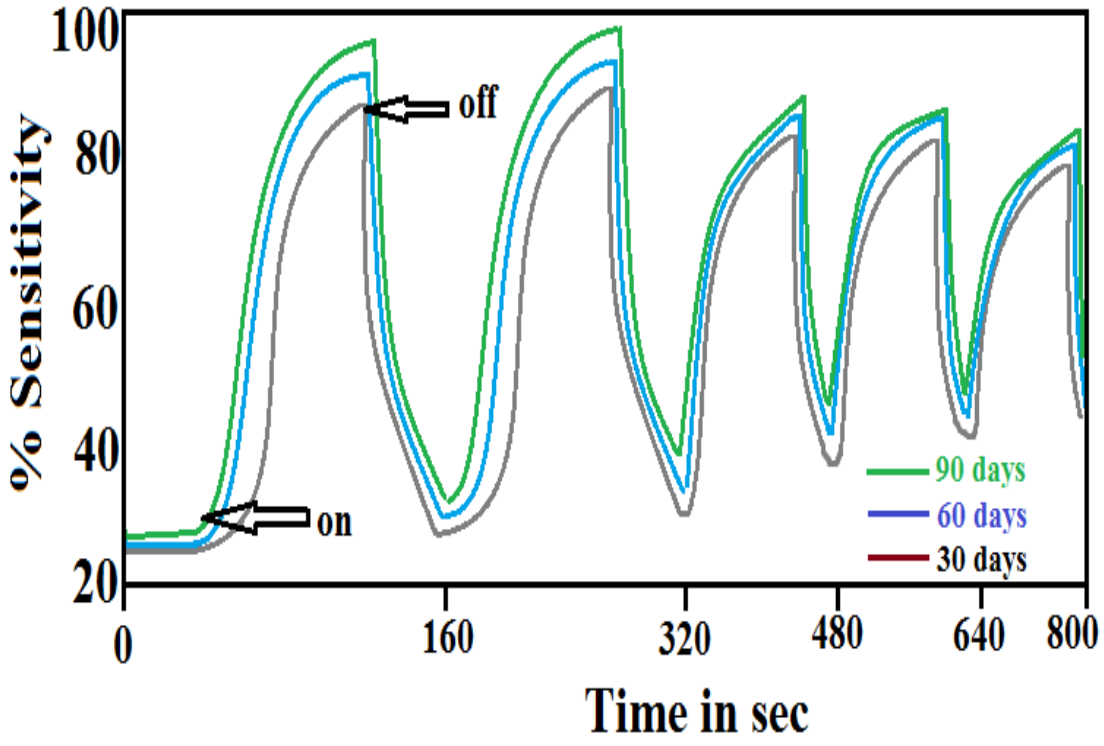

Figure 11

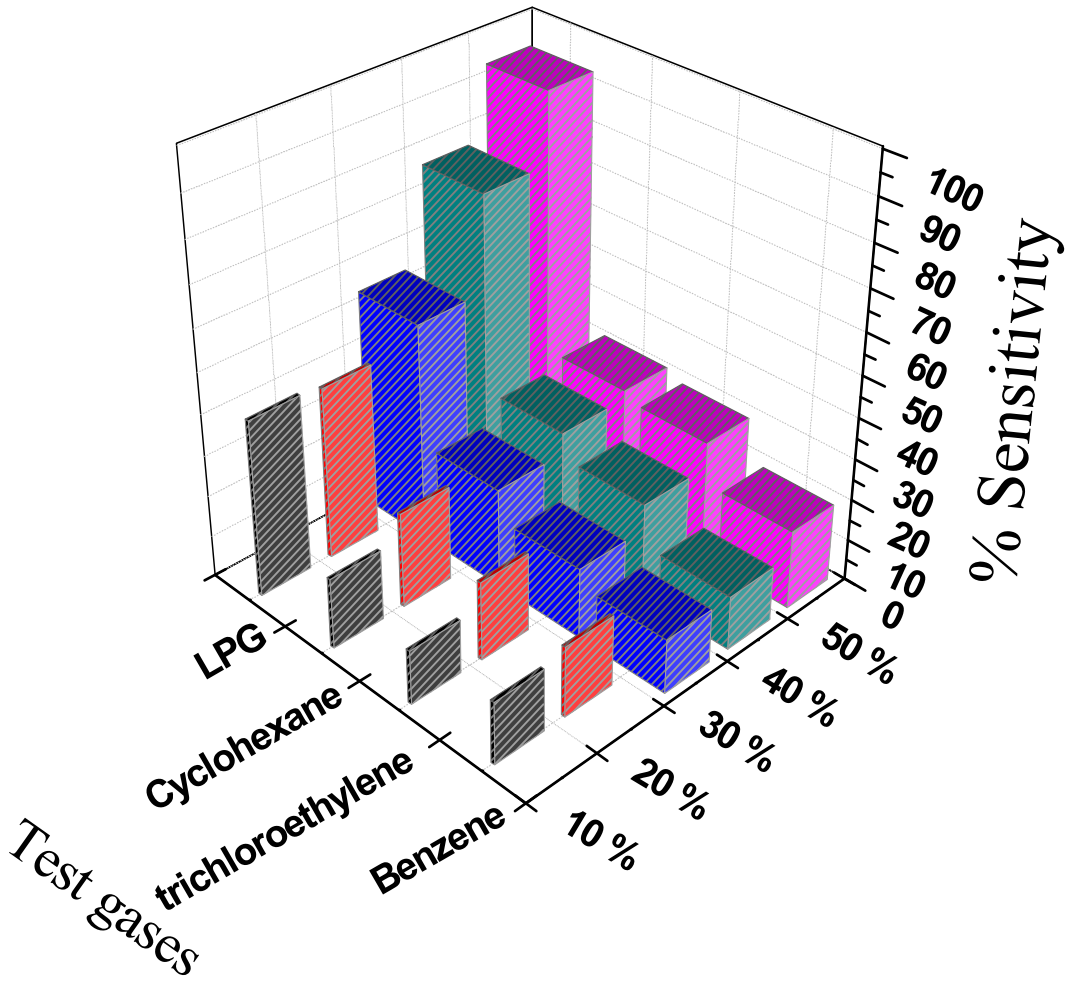

Figure 12

Table 1 Response and recovery times of OPANI and OPANI - ZnO nanocomposites for LPG

Sl.No	Details of the composites used OPANI/ZnO nanocomposites	Response time (t_{res}) in min at 400 ppm	Recovery time (t_{rec}) in min at 400 ppm
1	Ortho chloropolyaniline	39.91	71.54
2	10 wt. % nanocomposites	43.42	61.63
3	20 wt. % nanocomposites	42.17	69.07
4	30 wt % nanocomposites	50.80	62.16
5	40 wt % nanocomposites	46.29	71.36
6	50 wt % nanocomposites	56.76	37.59